Real-time measurement of lithium-ion batteries' state-of-charge based on air-coupled ultrasound

Cite as: AIP Advances **9**, 085116 (2019); https://doi.org/10.1063/1.5108873
Submitted: 03 May 2019 • Accepted: 11 August 2019 • Published Online: 20 August 2019

Jun-Jie Chang, Xue-Feng Zeng and Tao-Lei Wan

Real-time measurement of lithium-ion batteries' state-of-charge based on air-coupled ultrasound

Cite as: AIP Advances 9, 085116 (2019); doi: 10.1063/1.5108873
Submitted: 3 May 2019 • Accepted: 11 August 2019 •
Published Online: 20 August 2019

Jun-Jie Chang,[1,2,3,a] Xue-Feng Zeng,[1,2,b] and Tao-Lei Wan[1,2,c]

AFFILIATIONS

[1]Key Lab of Nondestructive Testing, Ministry of Education, Nanchang Hangkong University, Nanchang 330063, China
[2]Yangtze Delta Region Institute of Tsinghua University, Jiaxing, Zhejiang 314000, China
[3]Japan Probe, 1-1-14 Nakamura Chou Minami Ward Yokohama City, Kanagawa Prefecture 2320033, Japan

[a]junjiechang@hotamil.com
[b]**Correspondence:** abc997178163@gmail.com
[c]354442958@qq.com

ABSTRACT

In order to overcome the drawbacks of the traditional method of measuring a lithium-ion battery's state-of-charge by charging and discharging its voltage curve, a method based on air-coupled ultrasound is proposed, which slows aging of the battery. Analysis is conducted on the propagation characteristics of ultrasound in the battery using Biot's fluid-saturated porous media model; the signal is monitored in real time by monitoring ultrasonic waves during charging, and fast-wave and slow-wave signals are obtained. Firstly, the fast-amplitude value of the time domain signal is analyzed, and the near linear relation between the amplitude and lithium-ion battery's state-of-charge is established. Frequency domain analysis is then carried out to understand the relationship between the phase and phase velocity for different state-of-charge consumptions and spectra. The results from using an air-coupled ultrasonic detection method to obtain the fast-amplitude value of the battery's time domain signal show that fast-amplitude has an approximately linear relationship with state-of-charge. This verifies the feasibility and accuracy of this method and provides a new theoretical foundation for the real-time monitoring of lithium-ion batteries' state-of-charge.

I. INTRODUCTION

In recent years, with the vigorous development of lithium-battery-chemical technology, new energy-powered vehicles are gradually beginning to replace fuel vehicles. The nickel-cobalt-manganate-lithium battery (Li(NiCoMn)O2: NCM) with its low cost, high gram capacity, good safety, and other excellent characteristics is widely used in electric vehicles. An important parameter in an energy storage device, the state-of-charge (SOC) of a lithium battery directly affects its life and vehicle performance.[1,2] SOC is one of the most important parameters in a lithium battery management system (BMS) and is of great significance for evaluating lithium battery usage, service life, and slowing aging.[3–5] Using the BMS to estimate the SOC is very complicated, often involving complex algorithmic processing, and the hardware sensors of the BMS are expensive.[6–8] Therefore, it is necessary to find a low-cost and high-accuracy method for estimating the charged state of lithium batteries. At present, the commonly used electric quantity estimation methods include the open-circuit voltage (OCV) method, the ampere-hour integral method, and the Kalman filter algorithm.[6,9,10] The OCV method measures the voltage between the positive and negative poles of the battery, and the SOC is estimated according to the battery charging and discharging curve. However, this method is not conducive to on-line monitoring, while error in the time-integral method can lead to deviation in the result, and the Kalman filter algorithm suffers from being complicated. The parameters in the model need to be updated in real time to estimate the battery's electric quantity, which is difficult to be widely used.

Ultrasonic testing methods have enjoyed gradually increasing use in the estimation of the electric quantity state of lithium batteries in recent years due to their versatility, easy operation, and accurate results. Davies et al. used an ultrasonic contact method to

measure the arrival time and amplitude of the ultrasonic signal of a lithium-iron-phosphate battery (LiFePO4) through multiple charging and discharging cycles and obtained the relationship between the SOC and the state of health (SOH) of the battery.[11] Gold et al. used adhesions to bond a piezoelectric ultrasonic transducer to both sides of a lithium battery, and the ultrasonic contact method was used to monitor the charging and discharging process in real time, and a time-domain signal with a high signal-to-noise ratio and a high resolution was obtained. They expounded the relationship between the first transmitted longitudinal wave (fast wave) and the second transmitted longitudinal wave (slow wave) and the lithium battery's quantity of electricity, especially the relationship between the delay time of slow wave and the quantity of electricity.[12] Ladpli et al. used adhesions to bond piezoelectric ultrasonic transducers at both ends of the same side of lithium battery and used an ultrasonic guided wave method to conduct a series of studies on the SOC and SOH, obtaining good results.[13–15] This method couples the ultrasonic piezoelectric transducer to the surface of the battery in a bonding manner to obtain a time-frequency signal with a high signal-to-noise ratio. Despite the quality of such results, there are still drawbacks; that is, the method is difficult to apply to lithium battery production environment and the actual lithium battery use environment.

Air-coupled ultrasound is suitable for the nondestructive testing and evaluation of materials due to its non-contact, high efficiency, and completely nondestructive characteristics.[16–18] They are used in many fields, such as the viscoelastic evaluation of composites by air-coupled ultrasound, the detection of internal defects of lithium-ion batteries by air-coupled C scanning technology, the evaluation of the bonding strength and weak bonding structure of double-layer plate.[19–22] In recent years, air-coupled ultrasound technology has made great progress. Although there is a huge difference in the acoustic impedance between the tested material and air, the air-coupled ultrasonic detection signal has low signal-to-noise ratio (SNR) and long residual pulse compared with contact ultrasound, however with the development of special transducer for air-coupled ultrasound, its SNR and other aspects can basically meet the detection requirements. In the fabrication of lithium batteries, several layers of graphite are usually stacked together and filled with liquid electrolyte, so this structure conforms to fluid-saturated porous media. Based on Biot's theory of fluid-saturated porous media, this paper uses air-coupled ultrasound to detect the ultrasonic propagation behavior of a lithium battery during charging, as well as the electrical quantity, obtaining fast-wave and slow-wave time-domain signals. The relationship between the fast amplitude and electrical quantity of the battery is established, and the phase-spectrum-analysis method is used to analyze the phases and phase velocities of fast and slow waves in different SOCs. The approximately linear relationship between the ultrasonic time-domain signal amplitude and the electric quantity is obtained, which provides a new method for the SOC estimation of a lithium battery.

II. THEORY

A. Biot's model

Biot's prediction of ultrasonic propagation in fluid-saturated porous media has been verified and developed by many scholars. Slow waves generated by ultrasonic waves in such media have been observed, theoretically confirmed, and widely used in the study of porous materials.[23–26] For example, Biot's prediction has proved fundamental in measuring the following: ultrasonic attenuation coefficients, thermal and viscosity characteristic lengths, and surface acoustic impedance; Biot's prediction has also been instrumental in the evaluation of human osteoporosis in medicine.[27–32] Due to the different internal porosities and microstructures of different porous materials, slow-wave sound velocity characteristics vary.[33–35] Pride and Parra studied the ultrasonic propagation characteristics in multi-layered porous rocks using this theory.[36,37] Therefore, based on the above analysis, the theory is also applicable to the detection of NCM battery electric quantity by air-coupled ultrasound. Test results and analysis results will be given in subsequent chapters.

B. Phase spectrum analysis

Sachse and Pao used the ultrasonic penetration method to measure the ultrasonic group velocity and phase velocity in solids and proposed the phase spectrum analysis method (PSM).[33] Due to the nature of porous materials, high-frequency ultrasound experiences severe attenuation, while low-frequency ultrasound experiences a strong dispersion phenomenon. Background noise of layered medium and structure scattering of fast wave will affect the time domain waveform of slow wave. In addition, low amplitude of slow wave may even cause signal distortion due to dispersion. The most important thing is that the air-coupling ultrasonic longitudinal resolution is low, these reasons make it impossible to accurately get the velocity from the slow wave time domain waveform. The phase spectrum analysis method is used to reduce all kinds of influencing factors to obtain signal phase velocity values for analysis.

From the time domain waveform fast Fourier transform (FFT), the real part $F(\omega)$ and the imaginary part $G(\omega)$ are extracted; the phase spectrum $\varphi(\omega)=\tan(F(\omega)/G(\omega))$, and its value is $[-\pi, \pi]$. The detection waveform and the reference waveform were respectively obtained by placing and not placing lithium batteries between ultrasonic transducers; the phase spectrum ϕ of the tested material is given by:[38]

$$\phi = (-\phi_\omega) - (\phi_s) + 360\frac{f}{V_\omega}(L + V_\omega T_c), \tag{1}$$

where f is the center frequency of the transducer, Vω is the sound velocity in air, ϕ_ω is the phase spectrum of the reference waveform, and ϕ_s is the phase spectrum of the detected waveform. The detected waveform can be a slow wave or fast wave, L is the thickness of the material being tested, and T_c is the time difference between the extraction of the detected waveform and the reference waveform, that is, the time difference between the beginning of the two waveforms. The phase propagation coefficient is given by the following equation:

$$\beta = \frac{2\pi}{360\mathrm{L}}\phi = \beta_2 + 2\pi\left[1 + \frac{V_\omega T_c}{L}\right]\frac{f}{V_\omega}, \tag{2}$$

where

$$\beta_2 = \frac{2\pi}{360\mathrm{L}}[\phi_s - \phi_\omega] \tag{3}$$

Combining equations (2) and (3), the phase velocity can be calculated as:

$$V_p = \frac{\omega}{\beta} = \frac{V\omega}{1 + \frac{V_\omega T_c}{L} + \frac{V_\omega \beta_2}{2\pi f}}. \tag{4}$$

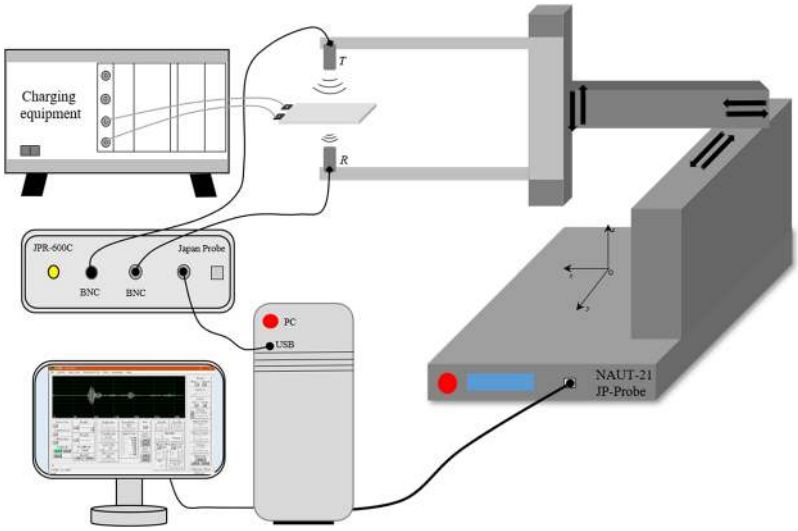

FIG. 1. The air-coupled ultrasonic NAUT-21 detection system.

The phase spectrum distribution and phase velocity values of fast and slow waves can be obtained by combining the above methods.

III. LABORATORY EQUIPMENT

An air-coupled ultrasonic NAUT-21 detection system was used and is shown in Fig. 1. The detection system consists of a high-power composite ultrasonic pulser/receiver (JPR600C), NI-PXI-5114 signal acquisition card, three-axis stepper motor, ultra-low noise receiver power amplifier, air-coupled dedicated transducer (provided by Japan Probe Co. Ltd.: Yokohama, Kanagawa Prefecture, Japan), and system control software. The lithium battery model is a CEA-LM36 (NiMnCoO2), with a rated capacity of 36 Ah, size 227×162×8.5 mm^3, and a rated voltage of 3.7 v. The transducer central batteries are arranged with 40 mm of spacing between them, and the temperature of the batteries is maintained at 25 °C; the charging voltage is kept constant, and online measurements at regular intervals are taken. Due to the high-frequency attenuation of ultrasound in the porous medium, the low frequency-dispersion is severe, and the residual vibration of the air coupled transducer is protracted; the lower the frequency, the more pronounced the effect, resulting in the aliasing phenomenon of fast and slow wave signals. Therefore, the integrated ultrasonic signal energy and signal resolution are selected using a couple of 400 kHz air-coupled ultrasonic transducers.

The ultrasonic pulses generate ultrasonic waves and are received by the receiving transducer through the air and the battery; then the received signal passes through the power amplifier to the ultrasonic pulser/receiver and the personal computer. In this experiment, the transmission voltage of the ultrasonic pulser is 300 V, and the sampling frequency is 20 MHz.

IV. EXPERIMENTAL RESULTS

A. Time domain analysis

The cell is placed in the center of the two transducers, which are perpendicular to the surface of the lithium battery; the waveform is collected during charging. Figure 2 shows the time-domain waveform of the signal when the lithium battery is at 100% and 25% power (gray line). Waveform ① is fast wave calculated by geometric acoustics. Waveform ③ is the reflected wave of waveform ① on the lower surface of the lithium battery; by combining porous media theory with waveform analysis, when the battery has a

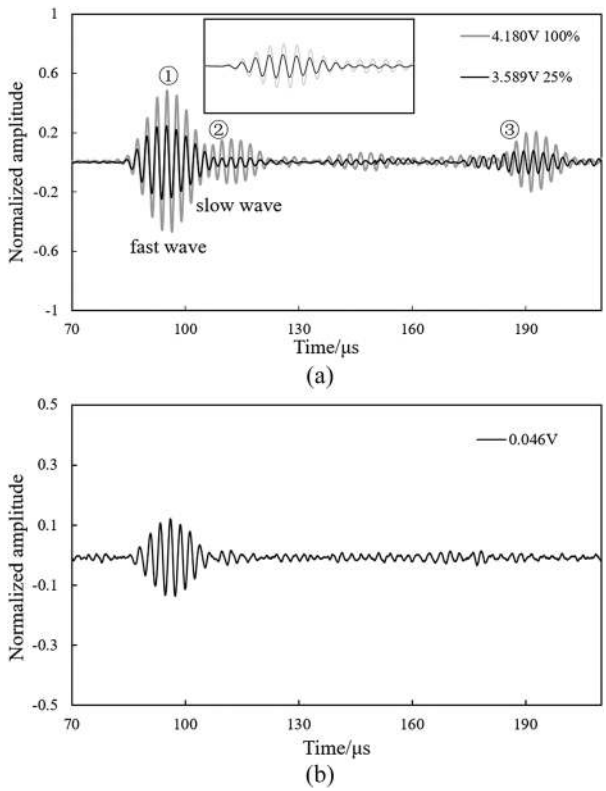

FIG. 2. Fully charged and 25% charged time domain signal. (a) The gray curve is the full charged time domain signal and the black curve is the 25% SOC time domain signal; (b) Time domain signal at open circuit voltage of 0.046v.

different electric quantity, waveform ② becomes the slow wave. The fast amplitude reaches 0.484 (normalized amplitude) and the slow amplitude is 0.162 when the cell is fully charged; the fast amplitude is 0.256 and the slow amplitude is 0.053 when the cell is at 25% charge, and the slow arrival time differs by 5.3 μs. This result is slightly different from the detection result of Gold; that is, the amplitude of the fast wave will also change correspondingly with the electric quantity.[12] Factors such as the type, thickness, number of internal layers, and the structure of the lithium battery all lead to the same point and difference of the results. In the fully charged and low battery(10% power) state, the amplitude of the fast wave drops from 0.484 to 0.21. In order to verify the correctness and accuracy of this result, the author over-discharged the battery to attenuate the open circuit voltage to 0.046 V; the time domain waveform is shown in Fig. 2(b).

It can be seen from the results that the signal amplitude attenuated to 0.125, indicating that the amplitude of the fast wave changes with the change of the lithium battery's electric quantity under the condition of air coupled ultrasound. Figures 3(a) and 3(b) show the curves of fast-wave amplitude and slow-wave amplitude with varying SOC. The gray curve in Fig. 4 shows the relationship between the battery power of this model and the open circuit voltage of the battery; the black curve shows the relationship between the amplitude of the fast wave and the cell SOC. It can be seen from the results

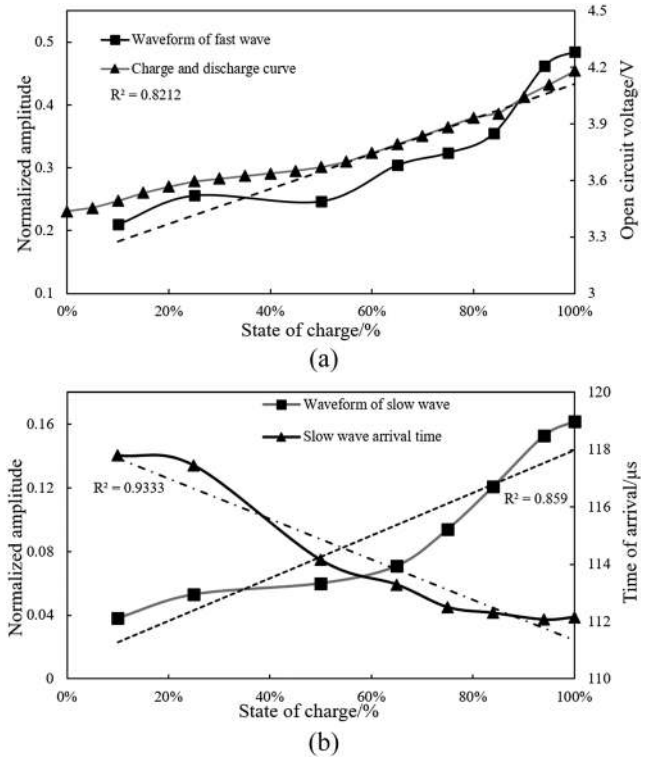

FIG. 3. Relationship between fast wave amplitude and power, slow wave amplitude and power and arrival time: (a) Gray curve: Charge-discharge curve; black curve: the relationship between fast amplitude and lithium battery charge; (b) Gray curve: the relationship between slow amplitude and lithium battery charge; black curve: the relationship between signal time of arrival and battery charge.

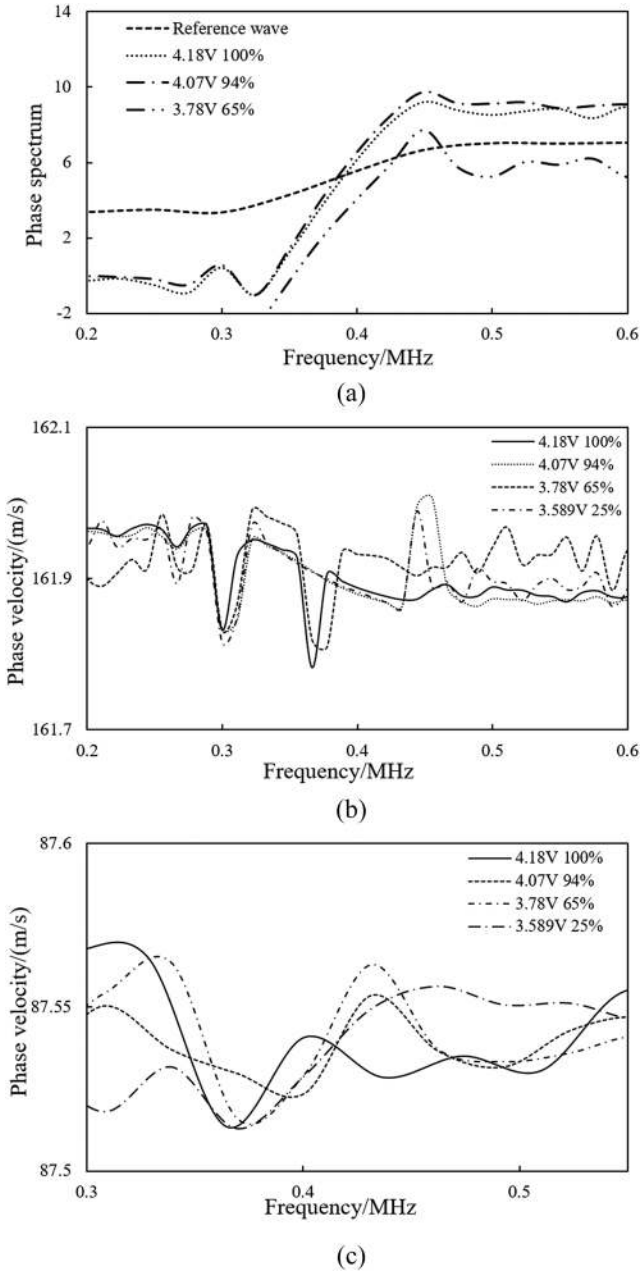

FIG. 4. Phase spectrum calculation result: (a) The fast wave phase spectrum of reference and different SOC waveform; (b) The phase velocity spectrum of the fast wave with different charges; and (c): The phase velocity spectrum of the slow wave with different electric quantities.

that the amplitude fluctuation of the fast wave is 0.274 and has a good linear dependence (R^2=0.8212) with electric quantity. The gray curve in Fig. 3(b) shows the relationship between the amplitude of the slow wave and battery power. The amplitude fluctuation is 0.124, and its linear dependence (R^2=0.8590) is more accurate than that of the amplitude of the fast wave; the black curve represents the

relationship between the arrival time of the slow wave and power (the arrival time fluctuation is 5.65 μs). Compared with the linearity between amplitude and power, the linearity between signal arrival time and power is higher (R2=0.9333). However, the charging process is accompanied by small and even microscopic bubbles, which cause a slight change in the thickness of the lithium battery. Air-coupled ultrasound is extremely sensitive to the gas bubbles, which will have an impact on the arrival time of the signal.

B. Frequency domain analysis

Fast and slow waves are analyzed in the frequency domain by using the phase spectrum method mentioned above, and their phase velocities are solved. For porous materials, it is important to analyze the fast and slow wave phase velocities. Figure 4(a) shows the phase spectrum of the waveform between the reference waveform and different electric quantities. The reference waveform trend is similar to the increasing and decreasing trend of the phase spectrum of the fast waves with varying electric quantity, fluctuating by 2.5 rad at the central frequency (400kHz) of the transducer. Figures 4(b) and 4(c) show the phase velocities of the fast and slow waves of different electric quantities, respectively, showing good consistency. The phase velocity of the fast wave fluctuates within the range of 0.3 m/s, and the phase velocity value at the central frequency is 161.89 m/s under the condition of full charge; the phase velocity of the slow wave fluctuates within the range of 0.04 m/s, and the phase velocity value at the central frequency is 87.54 m/s under the condition of full charge.

V. CONCLUSION

According to the above analysis, it is feasible to estimate the lithium battery power by using air-coupled ultrasonic detection method. Although the signal-to-noise ratio and resolution of signals are low due to many factors such as air-coupled ultrasonic transducers, slow waves are still observed in the NCM battery, and there is a nearly linear relationship between the amplitude of slow waves and fast waves and the lithium batteries' state of charge.

With the advantages of integrated air-coupled ultrasound, this method has great potential, opening a new field for the electric-quantity-state estimation of lithium batteries. Future work will involve how to improve the signal-to-noise ratio of the lithium battery during the detection process, accurately monitoring the state of charge of the lithium battery after multiple charging and discharging cycles, and monitoring the SOC of various types of commercial battery during charging and discharging.

ACKNOWLEDGMENTS

This project is supported by the National Natural Science Foundation of China (grant NO.11464030).

REFERENCES

[1] H. Yang, J. Zhang, and H. Zhang, Advanced Technology of Electrical Engineering and Energy **35**(01), 30–35 (2016).
[2] F. Feng, K. Song, R. Lu, G. Wei, and C. Zhu, Journal of Energy Storage **30**(01), 22–29 (2015).
[3] S. F. Schuster, T. Bach, E. Fleder, J. Müller, M. Brand, G. Sextl, and A. Jossen, Journal of Energy Storage **1**, 44–53 (2015).
[4] M. Ecker, N. Nieto, S. Käbitz, J. Schmalstieg, H. Blanke, A. Warnecke, and D. U. Sauer, Journal of Power Sources **248**, 839–851 (2014).
[5] L. Lu, X. Han, J. Li, J. Hua, and M. Ouyang, Journal of power sources **226**, 272–288 (2013).
[6] Y. Liu, S. Dai, Z. Cheng, and L. Zhu, Advanced Technology of Electrical Engineering and Energy **29**(01), 221–228 (2014).
[7] Y. Rong, W. Yang, H. Niu, and X. Zheng, Advanced Technology of Electrical Engineering and Energy **34**(09), 22–28 (2015).
[8] Y. Zheng, M. Ouyang, X. Han, L. Lu, and J. Li, Journal of Power Sources **377**, 161–188 (2018).
[9] H. Deng, Y. Deng, and H. Teng, Instrumentation Technology **02**, 21–24 (2015).
[10] F. Yao, N. Zhang, and K. Huang, Journal of Power Supply, 1–12, http://kns.cnki.net/kcms/detail/12.1420.TM.20190321.1324.004.html.
[11] G. Davies, K. W. Knehr, B. Van Tassell, T. Hodson, S. Biswas, A. G. Hsieh, and D. A. Steingart, Journal of The Electrochemical Society **164**(12), A2746–A2755 (2017).
[12] L. Gold, T. Bach, W. Virsik, A. Schmitt, J. Müller, T. E. Staab, and G. Sextl, Journal of Power Sources **343**, 536–544 (2017).
[13] P. Ladpli, F. Kopsaftopoulos, and F.-K. Chang, Journal of Power Sources **384**, 342–354 (2018).
[14] P. Ladpli, C. Liu, F. Kopsaftopoulos, and F.-K. Chang, presented at the 2018 IEEE Transportation Electrification Conference and Expo, Asia-Pacific (ITEC Asia-Pacific), 2018 (unpublished).
[15] P. Ladpli, F. Kopsaftopoulos, R. Nardari, and F.-K. Chang, presented at the Smart Materials and Nondestructive Evaluation for Energy Systems 2017, 2017 (unpublished).
[16] Z. Zhou and W. Dong, Chinese Journal of Mechanical Engineering **06**, 10–14 (2008).
[17] M. Castaings and B. Hosten, Ndt & E International **34**(4), 249–258 (2001).
[18] J. Chang, C. Lu, and Y. Ogura, Nondestructive Testing Technology **37**(04), 6–11 (2013).
[19] X. Zeng, J. Chang, C. Lu, G. Li, and G. Luo, Journal of Applied Acoustics **38**(01), 105–113 (2019).
[20] J. Chang, K. Yang, G. Li, and X. Zeng, Battery Bimonthly **47**(05), 315–317 (2017).
[21] X.-G. Wang, W.-L. Wu, Z.-C. Huang, J.-J. Chang, and N.-X. Wu, Materials **11**(2), 310 (2018).
[22] W.-L. Wu, X.-G. Wang, Z.-C. Huang, and N.-X. Wu, AIP Advances **7**(12), 125316 (2017).
[23] T. J. Plona, Applied Physics Letters **36**(4), 259–261 (1980).
[24] J. G. Berryman, Applied Physics Letters **37**(4), 382–384 (1980).
[25] M. A. Biot, The Journal of the Acoustical Society of America **28**(2), 168–178 (1956).
[26] M. A. Biot, The Journal of the Acoustical Society of America **28**(2), 179–191 (1956).
[27] M. Herskowitz, S. Levitsky, and I. Shreiber, Ultrasonics **38**(1-8), 767–769 (2000).
[28] N. Brown, M. Melon, V. Montembault, B. Castagnède, W. Lauriks, and P. Leclaire, Comptes rendus de l'Académie des sciences. Série IIb, Mécanique **322**(2), 122–127 (1996).
[29] F. Fohr, D. Parmentier, B. R. Castagnede, and M. Henry, Journal of the Acoustical Society of America **123**(5), 3118 (2008).
[30] P. Leclaire, L. Kelders, W. Lauriks, C. Glorieux, and J. Thoen, The Journal of the Acoustical Society of America **99**(4), 1944–1948 (1996).
[31] D. Lafarge, J. F. Allard, B. Brouard, C. Verhaegen, and W. Lauriks, The Journal of the Acoustical Society of America **93**(5), 2474–2478 (1993).
[32] Z. E. Fellah, N. Sebaa, M. Fellah, F. G. Mitri, E. Ogam, W. Lauriks, and C. Depollier, IEEE Transactions on Ultrasonics, Ferroelectrics, and Frequency Control **55**(7), 1508–1515 (2008).

[33]W. Sachse and Y. H. Pao, Journal of Applied Physics **49**(8), 4320–4327 (1978).
[34]Y. Bouzidi and D. R. Schmitt, Journal of Geophysical Research: Solid Earth **114**(B8) (2009).
[35]T. G. Alvarez-Arenas, L. E. Segura, and E. R.-F. de Sarabia, Journal of Applied Physics **78**(4), 2843–2845 (1995).
[36]S. R. Pride, E. Tromeur, and J. G. Berryman, Geophysics **67**(1), 271–281 (2002).
[37]J. O. Parra and P. c. Xu, The Journal of the Acoustical Society of America **95**(1), 91–98 (1994).
[38]T. G. Alvarez-Arenas, E. R.-F. de Sarabia, and F. M. de Espinosa-Feijo, Ultrasonics **32**(2), 131–140 (1994).